Journal of Constructional Steel Research 71 (2012) 92–103

Contents lists available at SciVerse ScienceDirect

Journal of Constructional Steel Research

Steel plate shear wall with tension-bracing for seismic rehabilitation of steel frames

M. Kurata [a,*], R.T. Leon [b], R. DesRoches [b,c], M. Nakashima [a]

[a] Disaster Prevention Research Institute, Kyoto University, Gokasho, Uji, Kyoto, 611-0011, Japan
[b] School of Civil and Environmental Engineering, Georgia Institute of Technology, Atlanta, GA 30332-0355, United States
[c] College of Engineering, Georgia Institute of Technology, Atlanta, GA 30332-0355, United States

ARTICLE INFO

Article history:
Received 24 May 2011
Accepted 29 October 2011
Available online 6 December 2011

Keywords:
Seismic rehabilitation
Thin steel plate
Shear wall
Tension bracing
Finite element model

ABSTRACT

A rehabilitation technique that utilizes a thin steel plate as a supplemental shear wall system for small, low-rise steel structures is described. In the proposed system, the plate and surrounding boundary elements are installed in the middle of the bay, separate from existing columns. This geometry intends to eliminate the need to strengthen the existing columns, as these typically would have been designed only for the combined forces of gravity and wind. The system employs supplemental elements as tension-only elements to speed up the construction work and to enforce strict capacity design principles (*i.e.*, overstrength is capped). A prototype system was designed using a hierarchical flowchart and a simplified analysis model, and its performance was evaluated through large scale testing. The system achieved stable hysteretic behavior without showing major strength deterioration until large story drifts were reached. A high-fidelity FE model of the system was also developed to reproduce the experimental behavior. The model well traced the test results and was used as a tool for validating the effectiveness of the proposed system geometry.

1. Introduction

The need to retrofit in earthquake prone regions may arise directly from the problem of aging infrastructure, recognition of the vulnerability of existing infrastructure, updates in seismic code requirements, or changes in building performance objectives. The addition of seismic isolation, supplemental bracing, concrete or steel shear walls, and damping devices are some common techniques that have been successfully implemented for improving the seismic performance of existing buildings (*i.e.*, improving stiffness, strength and energy dissipation). However, if the proposed modification results in the need for extensive additional strengthening of existing structural elements, rehabilitation may no longer be a cost-effective alternative to rebuilding. This is particularly true for small, low-rise steel structures, which are the target of the system described in this paper. Thus, the design of the supplemental system must follow a strict capacity design to avoid the major increase in force demand to the existing frames. Moreover, use of heavy construction equipment must be limited or eliminated in order to minimize indirect construction costs and mitigate safety concerns.

In response to these constraints, an approach to design supplemental systems utilizing tension-only elements is proposed for small to mid-sized buildings. The tension-only design can increase the speed of construction by adopting simple connections with rapid and adjustable installation features [1,2]. Such systems rationally implement a strict capacity design philosophy (over-strength is known or capped) and is scalable and adaptable to many bay geometries by eliminating undesirable global and local buckling in supplemental elements. In this paper, the adoption of a steel thin plate within a tension-only design approach is considered. A shear wall made of a steel thin plate resists lateral loads by developing tension field action after the onset of global shear buckling. Such a system, labeled a Special Plate Shear Wall (SPSW), is lighter and more ductile than a reinforced concrete shear wall and can provide the system with a substantial increase in stiffness, load-carrying capacity, and energy dissipation. Since Thorburn et al. [3] introduced the design philosophy for the use of unstiffened thin plates and considered the post-buckling strength of the infill plate for the calculation of shear strength of system, this new design philosophy has been widely adopted by researchers and in the current design codes (*e.g.*, [4–11]). While the SPSW is economical and efficient for increasing the seismic resistant capacity of steel moment frames, this system also significantly increases the force demand in boundary elements (*i.e.*, beams and columns) since inward flexural forces induced by the tension field action in a thin steel plate must be resisted by the flexural bending of boundary elements. This problem has led designers to propose alternative designs to lessen the increase in force demand to the existing frames.

This paper proposes an alternative configuration for SPSWs, where a plate with surrounding boundary elements is installed at the middle of the bay, separate from existing columns. The system incorporates stiffening of vertical boundary elements by tension-rods to ensure stable energy dissipation through the yielding of the thin steel plate

* Corresponding author. Tel.: +1 734 615 8177; fax: +1 734 764 4292.
E-mail addresses: kurata.masahiro.5c@kyoto-u.ac.jp (M. Kurata), roberto.leon@ce.gatech.edu (R.T. Leon), reginald.desroches@ce.gatech.edu (R. DesRoches), nakashima@archi.kyoto-u.ac.jp (M. Nakashima).

0143-974X/$ – see front matter © 2011 Elsevier Ltd. All rights reserved.
doi:10.1016/j.jcsr.2011.10.026

while limiting the dimension of the boundary elements. The paper first provides an overview of the design approach and prototype design. This discussion is followed by performance validation of the prototype in a large scale test. Finally, a FE model of the proposed system is developed and validated using the test results.

2. Concept of steel plate shear wall with tension-bracing

The schematics of a conventional SPSW system and the proposed Shear Wall system with Tension-Bracing (SW-TB) are described in Fig. 1. In conventional SPSWs, a steel thin plate is welded or bolted to the surrounding boundary elements. When a lateral load deforms the framing, the infill plate starts to develop a tension field after the onset of global buckling, and the inward force induced by the tension field action is resisted by the bending rigidity of the boundary elements. The boundary elements, especially the vertical boundary elements (VBEs) require sufficient stiffness and strength to ensure extensive yielding of the infill panel. If the failure mode of a steel thin plate shear wall system is governed by the capacity of boundary elements, only a negligible increase in system strength is achieved and the excess plate material used is wasted. Lubell et al. [12] reported such test results for the SPSW, where inward flexure of boundary elements resulted in an hourglass effect with only a limited area of tension field action developing in the infill panel. Similarly, Behbahanifard et al. [8] reported test results which involved severe damage in VBEs due to local flange buckling. Qu et al. [13] proposed on flexibility limits for VBEs design by reviewing the derivation of a flexibility factor in plate girder theory and how that factor was incorporated into current codes. These reports also highlighted the severe load condition in the VBEs (*i.e.*, columns) in the SPSW system.

An additional design problem is that the available steel plate material often leads to thicker or stronger SPSWs than required by design. According to capacity design principles, this overstength is undesirable as it may lead to unexpected failure modes of the structure. Several solutions proposed to address this issue include systems utilizing light-gauge cold-rolled and Low Yield Strength (LYS) steel [14,15]. Roberts, Vian and Purba also investigated the behavior of unstiffened thin steel pate shear walls having openings on the infill plate analytically and experimentally [15–17]. Hitaka and Matsui [18] thoroughly studied a steel plate shear wall with vertical slits where the steel plate segments between the slits behave as a series of flexural links, which provide a fairly ductile response without the need for heavy stiffening of the wall.

In the proposed system, the infill plate is positioned in the mid span away from existing columns. In response to the necessity in providing VBEs with enough strength and stiffness relative to the infill steel plate, the design of VBE as a pin-ended weak beam supported by tension-bracing elements is proposed. This approach avoids the need to install a strong beam as a conventional, full-bay VBE installation would require. In this configuration, the tension-rods attract a large amount of the inward force in the VBE and transfer them to beam elements of existing framings. The strength of the proposed system is controllable with the thickness of the infill panel and the width of the shear wall as well since the wall does not need to span the full-bay width.

2.1. Design description

The primary structural components of the proposed system are an infill panel, vertical boundary elements (VBEs), horizontal boundary elements (HBEs), tension-rods, and brackets (Fig. 2). Two tension-rods are placed at each corner, with one end of each rod attached to the VBEs at an inclination of 45°; eight tension-rods are used in total. The other ends of the tension-rods are anchored to beams at a position outside the protected zones (one half of beam depth away from column faces). The brackets shown in the figure were designed with the intent of limiting the force demand in the tension-rods through inelastic deformation at their connection to the VBEs. At the location of the brackets, the tension-rods also constrain the rotational movement of the VBEs and add to the additional stability in the system. The location of the brackets is pre-determined based on preliminary analyses and is intended to minimize the dimensions of the tension-rods and brackets while efficiently stiffening the VBEs.

A main design constraint for the prototype system is the requirement that yielding of the infill panel should occur prior to yielding of the boundary elements. The VBE will be subjected to inelastic deformation after this occurs due to the inward flexural force induced by the tension field developed in the infill panel. The tension-only elements are designed to remain elastic until very large deformations are reached. The design of the VBE requires an iterative procedure since its behavior interacts with the behavior of the tension-only rod and the local geometry of the bracket. The strength and stiffness of the VBEs greatly affect the global behavior of the system while

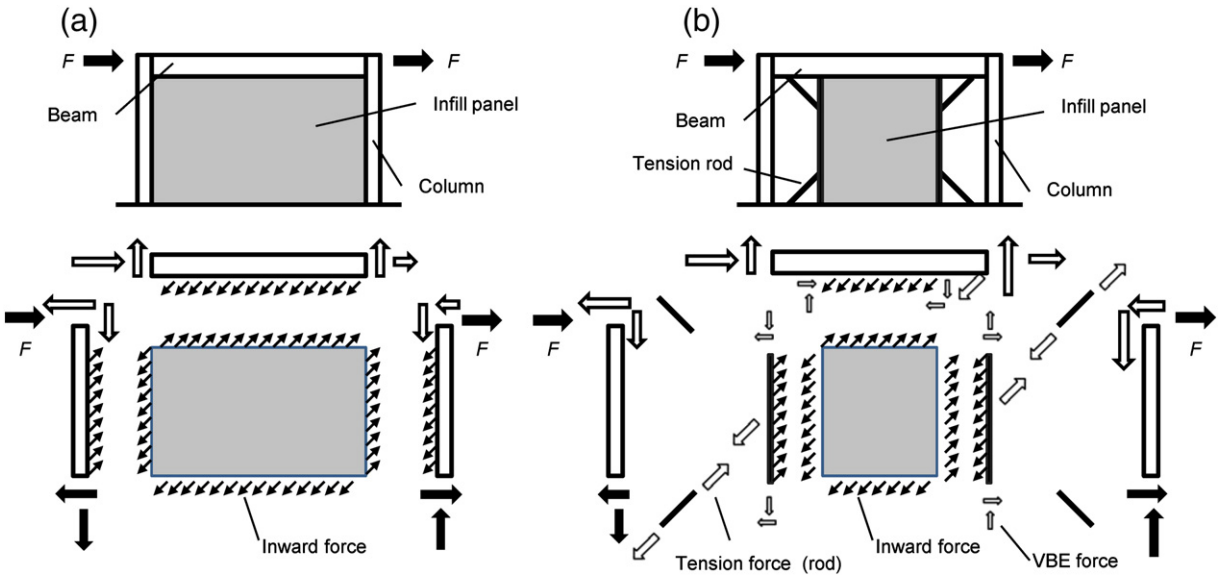

Fig. 1. Concept and free-body diagram of steel thin plate shear wall systems: (a) SPSW; and (b) proposed SW-TB system.

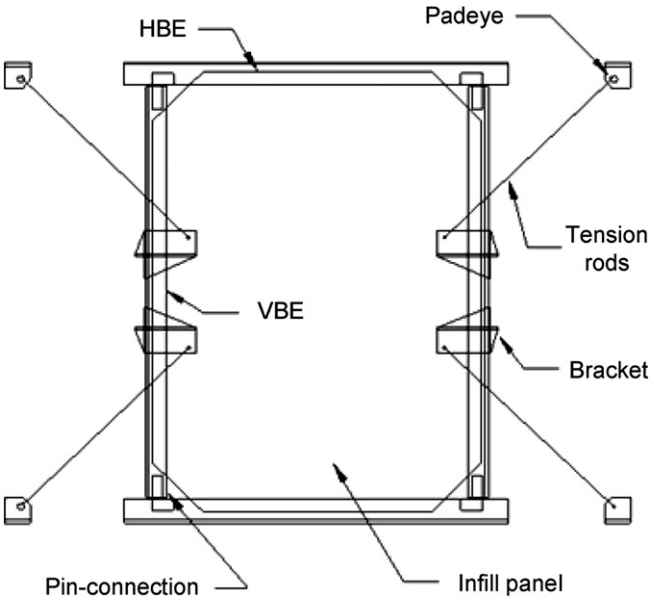

Fig. 2. Components of prototype.

the behavior of the HBE does not influence the global behavior as long as the VBEs are designed to be stronger than the infill panel; the proper design of the HBEs is a relatively easy task since they are directly attached to the top and bottom beams of a frame. Note that the VBEs can be designed with non-compact members since they do not carry large axial compressive load; the system expect the existing vertical load carrying member (columns) to carry vertical load.

2.2. Simplified analysis model

The design parameters in the prototype are determined by parametric analyses using a simplified analysis model (Fig. 3). The infill panel is modeled using a strip model in which an infill panel is represented by a series of inclined pin-ended tension-only members [3,19]. The strip analysis method has been shown, through correlation with physical test data, to adequately predict SPSW performance [10,11]. As the initial step, a simple model in OpenSEES [20] was used to develop the preliminary design. Although this simplified, uncalibrated model does not predict the behavior of the proposed system accurately, it provides both a rough estimate of the system shear strength and insights into the appropriate selection of design parameters.

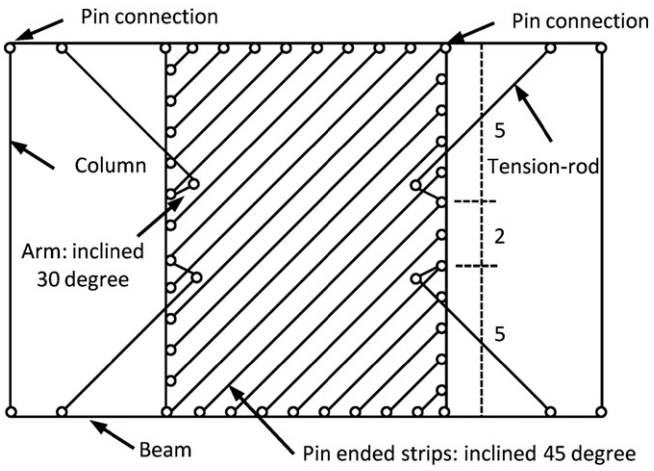

Fig. 3. Simplified analysis model.

In the strip model, the cross-sectional area of each strip is equal to the strip spacing times the panel thickness;

$$A_s = t_w(L\cos\alpha + H\sin\alpha)/n \tag{1}$$

where, t_w = thickness of panel, L = width of panel, H = height of panel, α = the inclination of the tension field and n = number of strips per panel. The tension-only strips are modeled by *truss* elements with a tension-only option. The inclination of the tension field is assumed as 45° since there is little experimental data available for the proposed geometry.

The tension-rods are connected to the VBEs with brackets each of which rigidly connects the rod end and the VBE with an inclination of 30°. The location and inclination of the arms are determined from preliminary analyses and by using reasonable engineering judgment. The prototype system has the brackets at five-twelfth and seven-twelfth height. The reasonable range of the location of the brackets are the locations from one-third and two-third to the mid height while the brackets need to be placed apart from each other to expect inelastic deformation at their connection to the VBEs. In the analysis, the arms are treated as rigid members using *elasticBeamColumn* elements with large stiffness. Beams and columns are modeled by *nonlinearBeamColumn* elements with *Steel02* material which is used to construct a uniaxial Giuffre-Menegotto-Pinto steel material object [20]. The translational degrees-of-freedom of all nodes in the bottom beam are fixed and a static displacement is incrementally applied to both ends of the top beam until a target displacement is reached.

2.3. Design flowchart

The design flowchart describes the iterative design procedure for the proposed SW-TB system (Fig. 4). Given the geometry of a frame and a target shear strength (V_n) for the proposed system, the approximate thickness of an infill panel is estimated using the formula specified in the U.S. and Canadian seismic codes for the calculation of the nominal shear strength of infill panel for SPSW system [10,11]. This formula includes an overstrength factor of 1.2;

$$t_w = V_n/0.42F_yL\sin 2\alpha \tag{2}$$

where, F_y = yielding stress of the infill panel, t_w = thickness of the infill panel, L = distance between the centerlines of VBEs and α = the inclination of the tension field. It should be noted here that this equation is valid when the aspect ratio of the infill panel is larger than 0.8 and the boundary elements satisfy the specified stiffness limitation [13,21]. The shear strength of the infill panel is used as a rough estimate of the total shear strength of the system since the pin connected boundary elements do not carry shear force. The inclination of the tension field is assumed to be 45°.

Once the thickness of the infill panel has been selected, a trial section is picked for the VBEs. In the first nonlinear static pushover analysis, the behavior of tension-rods is assumed to be elastic. Reasonable dimensions are assigned to tension-rods and arms. Using the analysis results, the requirement that the infill panel yields prior to the VBEs is checked. This judgment is rather arbitrary since not all areas of the infill panel yield even with very stiff and strong VBEs. For the design of the prototype, the criterion adopted is whether approximately 60% or larger area of the middle part of the infill panel has yielded or not; this criterion is intended to achieve the yielding of the plate along its entire height after one cycle of pushover and reversed loadings. When the criterion is satisfied, the diameter of the tension-rods is selected based on the force at the temporary target value of 1% story drift for simplifying the design process. A second analysis is then executed to see if the total shear strength of the system is acceptable. If the error is within a reasonable tolerance, the dimension of the arm is determined in an iterative manner to ensure that the

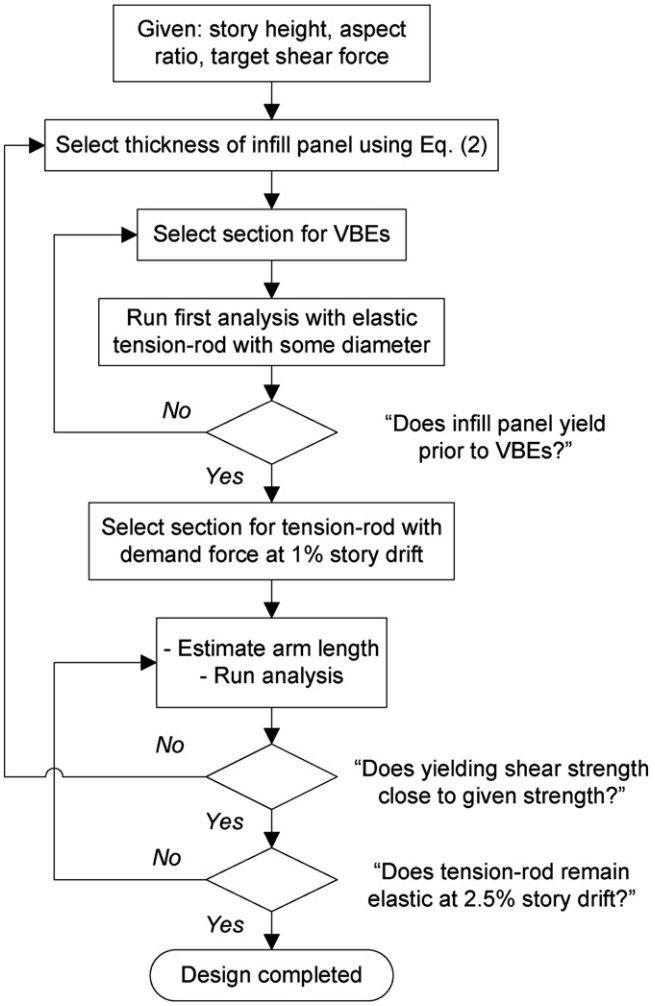

Fig. 4. Design flowchart.

tension-rod remains elastic to at least a 2.5% story drift; otherwise the thickness of the infill panel needs to be increased. The target story drift of 2.5% was defined to maintain the strength of the shear wall system under very large deformations above the design drift limit specified in ASCE 7.

2.4. Prototype design

The performance goal of the prototype was set to achieve a total system shear strength of 700 kN. This is approximately equal to the shear force carried by a three-bay frame in a typical low-rise steel moment resisting frame in Japan. This type of frame, with a Japanese standard section, H-250×250×9×14 (section modulus, Z_x = 860 cm^3, roughly equivalent to an American W12×40 section) for the columns, can sustain approximately 150 kN base shear if (a) it reaches its plastic moment capacity (M_p) at both ends, (b) the expected yield strength is taken as F_{ye} = 305 MPa (or 1.3 times its nominal value of 235 MPa) and (c) the story height of a frame to be rehabilitated is assumed to be 4 m (clear story height = 3.5 m). The aspect ratio of the infill panel is arbitrarily taken as 4:3 (height to width). The story height of a frame to be rehabilitated is assumed to be 4 m with its clear height as 3.5 m.

2.4.1. Prototype hysteresis

The selected thickness of the infill panel was 3.2 mm and the required section for the VBEs were defined as CT-200×200×8×13 (I_x = 1390 cm^4, Z_x = 88.6 cm^3, roughly equivalent to an American WT6×22.5 section in terms of section modulus). The expected yield strength of the infill panel made from a hot-rolled thin steel plate was assumed to be 207 MPa. The tension-rods were M30 with at a yield strength of 234 kN. The global hysteresis of the system in terms of shear strength versus story drift is shown in Fig. 5(a). The system yielded at approximately 0.50% story drift at a shear strength of 675 kN. The yield shear strength was estimated from the bi-linearization of the hysteresis curve as indicated in the figure. The hysteresis of the tension-rods located in the extended and shortened diagonals in the frame are shown in Fig. 5(b). In the pushover analysis, the rods located in the extended diagonal carried a large tension force as expected while the rods located in the shortened diagonal remained to carry a slight tension force. All rods remained elastic until 2.50% story drift as envisioned in the design approach.

2.4.2. Prototype design review

The following steps summarize the procedure to determine a satisfactory trial design:

1. The target shear strength of the prototype was 700 kN. The clear story height of a frame was 3.5 m and the aspect ratio of the infill panel was 4:3 (height-to-width).
2. The nominal shear strength of the panel was taken as F_y = 200 MPa. The thickness of the infill panel selected from inventory was 3.2 mm:

$$V_n = (0.42)(200)(3.2)(3500 \times 0.75)\sin 90^\circ/1000 = 706 \text{ kN}$$

The area of each strip in the simplified model was calculated as:

$$A_s = (3.2)(2625\cos 45^\circ + 3500\sin 45^\circ)/693 \text{mm}^2$$

3. Fig. 6(a) shows the shear strength of the system and the hysteresis of the strips in the middle part of the infill panel with four different sections of the VBEs; CT-150×150×6.5×9 (CT-150, Z_x = 33.8 cm^3), CT-175×175×7×11 (CT-175, Z_x = 59.3 cm^3), CT-200×200×8×13 (CT-200, Z_x = 88.6 cm^3), and CT-225×200×9×14 (CT-225, Z_x = 124 cm^3). The yield strength doubled when the section was changed from CT-150 section to CT-200 section. The yield shear strength with CT-200 section

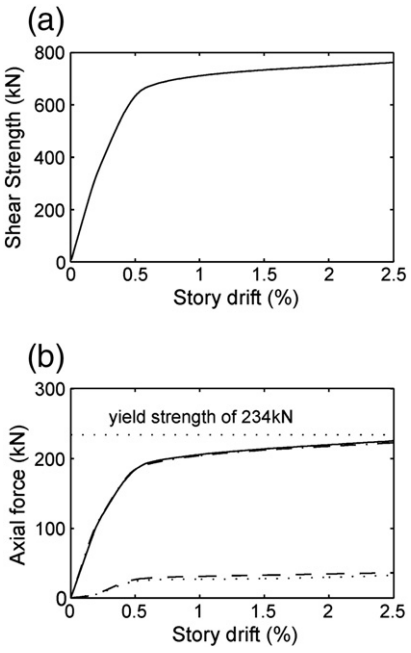

Fig. 5. Prototype behavior: (a) shear strength; (b) force history in tension-rods.

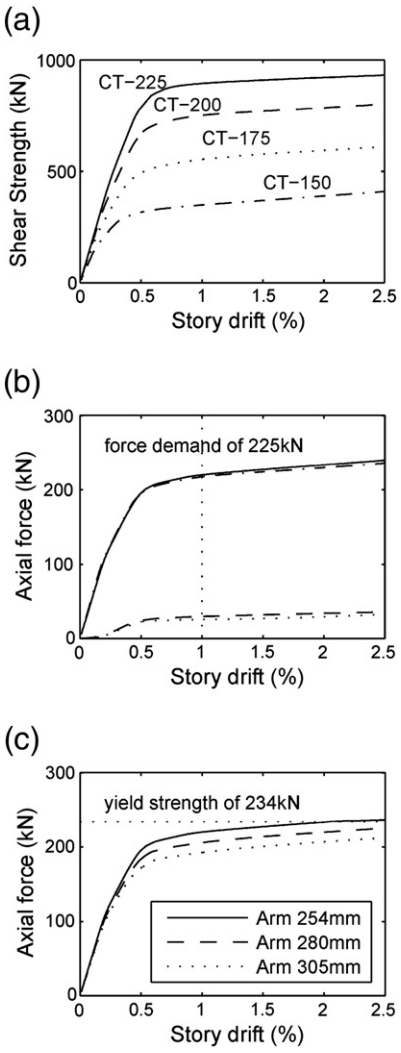

Fig. 6. Prototype design review: (a) shear strength with different VBEs; (b) tension-rod selection; and (c) arm length selection.

was approximately 725 kN which was slightly larger than the target shear strength. With the CT-175 section, only 1 strip yielded prior to the yielding of VBEs. The numbers of the yielded strips prior to the yielding of the VBEs increased significantly with CT-200 section and CT-225 section. Table 1 summarizes the estimated yield shear from bi-linearization of the hysteresis curves with various sections. The increase of section modulus affected significantly to the shear strength when the section was increased from CT-150 to CT-200. Once the shear strength of system was governed by the shear strength of the infill panel, the increase of section size did not lead to significant increase of the system shear strength. The CT-200 section was selected for the section of VBEs in the prototype. Here, the tension-rods were treated as elastic elements and the length of the arm was arbitrarily set to 280 mm.

4. The size of the tension-rod was defined based on the elastic force demand at 1% story drift, which was 225 kN [Fig. 6(b)]. In the figure, the rods carrying larger forces were located in the extended diagonal of the frame and the others were located in the shortened diagonal of the frame. The size of the rods selected was M30 with a yield strength of 234 kN.
5. The yield shear strength of the system was 710 kN and was close enough to the target shear strength. It was also notable that the yield strength was pretty close to the nominal yield strength of the infill panel (V_n) computed by the formula specified in the seismic codes.
6. The last step of the design was to define the length of the arm. Fig. 6(c) shows the force histories of tension-rods with the arm length of 254 mm, 280 mm and 305 mm. The length of 280 mm was required to remain the rods elastic at 2.5%.

Table 1
Yield shear strength for various sections.

Section	Z_x	Increase from Z_x of CT-150	Yield strength	Increase from yield strength of CT-150
	cm^3	%	kN	%
CT-150	33.8	0	300	0
CT-175	59.3	75	510	70
CT-200	88.6	162	725	142
CT-225	124	267	860	187

3. Experimental validation

The performance of the proposed system was evaluated through large scale testing at the structural laboratory of Kyoto University, Japan. The prototype was scaled to approximately 50% in a dimension for a proof-of-concept testing due to size limitations of the existing testing load frame. The target shear strength of the specimen was scaled down to 25% of the prototype strength, 150 kN. In the experimental program, two steel thin plate shear wall specimens were tested. One specimen had tension-bracing (specimen 2) and the other did not (specimen 1) in order to evaluate the effects of the bracing on the global and local behavior of the prototype. The test setup and specimens were fabricated using members and materials specified in Japanese standards.

3.1. Weld test for panel attachment

In the majority of past experiments, the infill wall was attached to the boundary elements via a continuous fillet welding method (*e.g.*, [9]). When welding is selected as the method for attachment, distortion and residual stresses in the thin steel panel become a concern. The distortion and residual stress are primarily caused by an angular bending of the plate itself due to the shrinkage of weld metal in unsymmetrical welds. For the case of SPSWs, Caccese et al. [6] reported a loss and nonlinearity in initial stiffness attributed to the slenderness of the infill plate; the imperfections in the plate due to fabrication cause out-of-plane deformations that commence almost immediately and the plate can sustain virtually no in-plane force without transverse movement. Elgaaly reported that the bolted plate shear walls had smaller elastic stiffness and lower initial yielding load than welded shear walls [7]. For a bolted plate, loss of initial stiffness can occur when the bolted connection starts slipping or when the plate yields locally near the boundaries. Steel plates thinner than 4.5 mm are available with the material as SPHC (Steel Plate Hot Commercial) or as SPCC (Steel Plate Cold Commercial) in the Japanese market. These materials are commonly used for mechanical engineering applications and contain more carbon and have surfaces smoother than typical structural steel. Because of the lower friction coefficients for this type of plate, the design of a bolted connection with these material properties require more bolts than that with a common structural steel, and thus weld connection were used to attach the steel thin infill panel to the boundary members.

3.1.1. Pre-holed fillet welding

The common strategy for welding a thin steel panel is a single path continuous fillet welding, as the angular distortion increses almost proportionally with the number of welding pathes [22]. As a plate become thinner, the welding around all edges should be completed in a

shorter amount of time since the distortion increases as the speed of welding decreases. However, the single path, continuous, and rapid welding technique demands high skilled and experienced welders and results in sacrifying the reliability of the weld strength. Alternatively, a fillet welding method utilizing a series of small holes ($\phi = 10$ mm) along the edges of the infill panel were proposed. This method limits the duration of each fillet welding process and reduces the input heat compared to single path fillet welding.

3.1.2. Preliminary weld test

Preliminary weld tests were conducted using the same thin steel plate as the infill panel in the test specimens. For comparison, the performance of a deep arc spot welding method was investigated as well. The main parameters in the preliminary weld tests were the method of weld, the posture of the welder, the weld size diameter and a weld pitch (Table 2). The dimension of specimen for the tensile test was 180×300 mm. The shape of a loading grip made of 9 mm A36 steel plate was designed specifically for the universal loading machine used in the tests [Fig. 7(a)]. The pitch of the location for welds was calculated using a minimum, long-term tensile strength of one spot weld specified in the manual [23].

All specimens except the specimen 10W2 which was pre-holed welded with a 10 mm diameter at the upright position, failed in the weld metal. Specimen 10W2 successfully failed by fracture of the thin plate [see the bottom specimen in Fig. 7(a)]. The shear strength per one weld obtained for different combinations of welding methods and welder's posture are summarized in Table 2. The specimen with a pre-hold fillet weld was 50% stronger than that with the deep arc spot weld for the same diameter. It was also notable that the pre-holed fillet weld in an upright posture was only 10% weaker than with a downward posture. Fig. 7(b) shows the test results for pre-hole welding specimens in terms of the force and displacement relationship. When failure occurred in the weld metal (7W4), the specimen failed in a brittle manner without any indication of post yielding deformation. The specimen showed large ductility if the failure occurred in the thin steel plate (10W2). Specimen 10W1 showed the combined behavior of two failure modes. The elastic stiffness of the specimen with the plate failure mode (10W2) was higher than that of the specimen with the weld failure mode (7W4 and 10W1).

3.2. Test setup and specimen

The test setup was a portal frame with four pins at each corner and has an inter-story height of 1748 mm and a column centerline spacing of 3000 mm. The lateral deformation of the test setup was controlled in a fully automated manner using the loading system which consists of a horizontal hydraulic jack, a hydraulic pump system and a control PC [Fig. 8(a) and (b)]. The main components of the testbed were: (a) top and bottom H-400×400×13×21 beams; (b) two H-250×250×9×16 columns; (c) four pin-clevis subassemblies with load carrying capacity of 900 kN each; and (d) a fixed support for the actuator loading. The assembly was capable of applying a horizontal force more than 750 kN, which was determined from the slip critical force at bolted connections. The deformation of the test setup was restrained to in-plane deformations using out-of-plane restrainers and guiding beams.

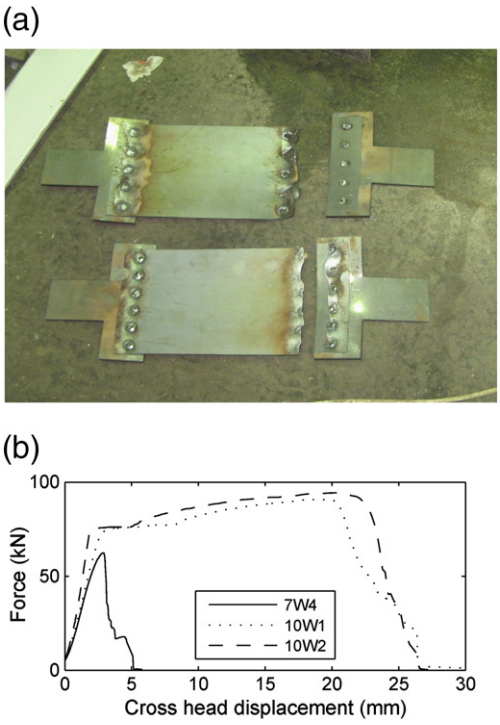

Fig. 7. Pre-holed weld test: (a) photo of specimens; (b) force displacement relationship.

Fig. 8(c) shows the geometry of the specimen determined following the design flowchart (Fig. 4). The thickness of the infill panel was selected as a 1.6 mm thin plate of low carbon mild steel (SHPC) with dimensions of 1250 mm×1673 mm. The required section for VBE was taken as CT-75×100×6×9 (SS400, $I_x = 51.7$ cm^4, $Z_x = 8.8$ cm^3). The section for HBE was CT-87.5×175×7.5×11 (SS400, $I_x = 115$ cm^4, $Z_x = 15.9$ cm^3). The required tension-rods were M16. The bracket consisted of mild steel plates (SS400) with thickness of 6 mm and 9 mm. At each corner, a VBE and HBE were connected using L-shape plates and high strength bolts [Fig. 8(d)]. This connection is designed to constrain translational and out-of-plane deformations and allows rotation at the connection similar to a pinned connection. The corners of the infill panel were cut to avoid interference with the connectors.

The typical assembly of a specimen was as follows: (1) HBEs were attached to the top and bottom beams of the test setup with high strength bolts, (2) VBEs were pin-connected to HBEs with L-shape plates and F10T-M16 high strength bolts, and (3) an infill thin steel panel was welded to the HBEs and VBEs. For the specimen with a tension-rod (specimen 2), the assembly continued as follows [Fig. 8 (d)]: (4) four steel brackets were installed to the VBEs using F10T-M14 high strength bolts, (5) four pad-eyes were bolted to the top and bottom beams, and (6) eight tension-bracing, composed of a

Table 2
Welding test results.

Specimen	Welding method	Welder's posture	Diameter	Pitch	Failure mode	Shear strength per weld	
			mm	mm		(kN)	(kip)
7W1	Deep arc spot	Look down	7	36	Weld metal fracture	8.2	1.80
7W2	Deep arc spot	Upright	7	36	Weld metal fracture	8.1	1.78
7W3	Pre-holed fillet	Look down	7	36	Weld metal fracture	12.5	2.75
7W4	Pre-holed fillet	Upright	7	36	Weld metal fracture	11.0	2.41
10W1	Pre-holed fillet	Upright	10	36	Weld metal fracture	15.5	3.41
10W2	Pre-holed fillet	Upright	10	30	Plate fracture	N/A	N/A

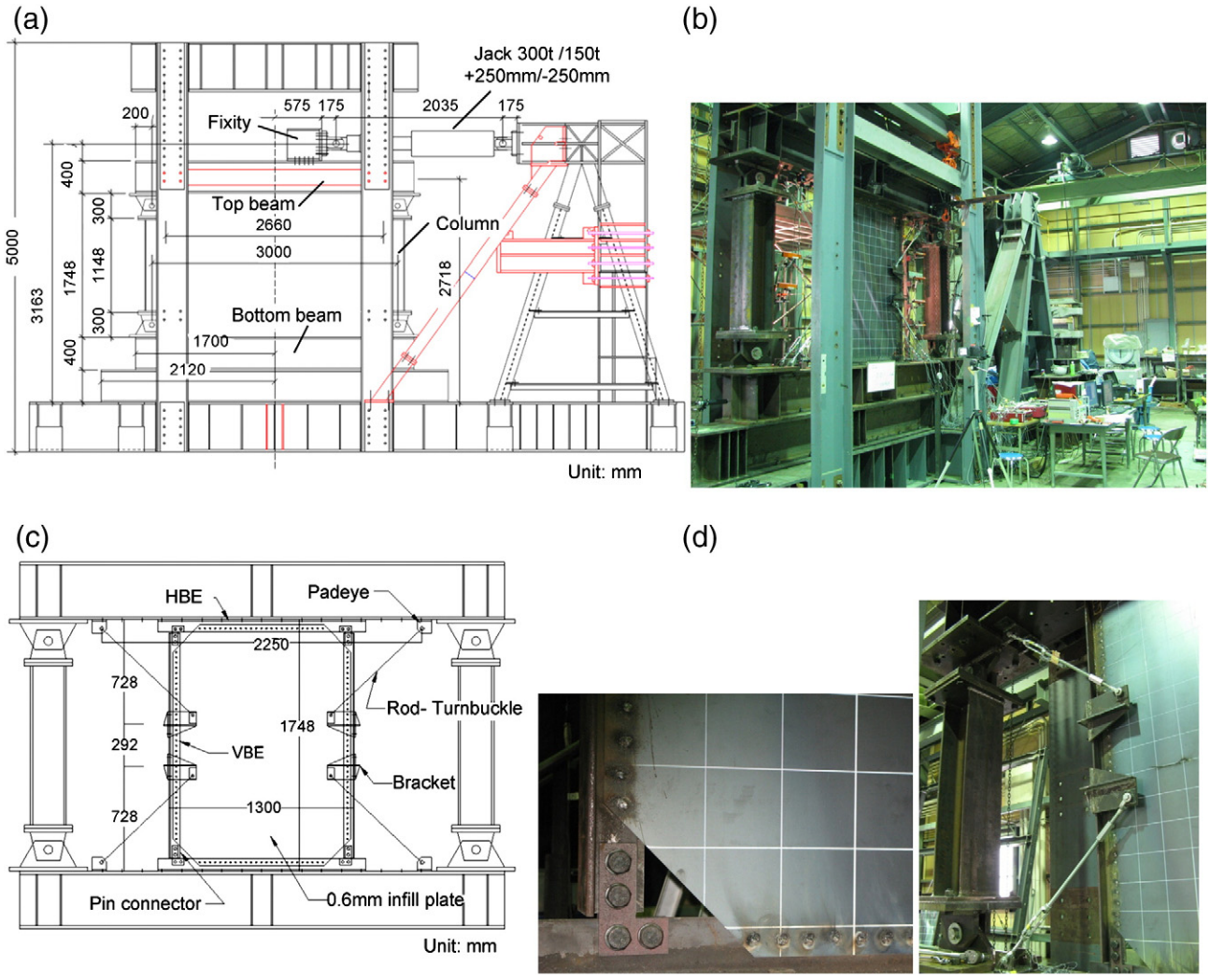

Fig. 8. Experimental setup: (a) loading frame; (b) photo of entire setup; (c) dimension of specimen with tension bracing; (d) (left) photo of pin-connector, (right) photo of tension-rod and bracket.

M16 steel threaded rod and a M16 steel turnbuckle, were connected the brackets and the padeyes.

3.3. Mechanical properties and test protocol

The mechanical properties of the infill panel, the web of the HBE, the flange and web of the VBE were obtained from tensile coupon tests and summarized in Table 3. The yielding and tensile strength of turnbuckles were obtained by tensile loading tests after the tests were completed. The shape of the coupons followed the Japanese Industry Standard [24].

The loading protocol used in the test consisted of 3 cycles at story drifts of 0.375%, 0.50% and 0.075%, followed by 2 cycles at 1%, 2%, 3% and 4% story drift. This loading protocol was determined after a review of the loading protocols used in previous tests and the design guidelines (*e.g.*, [11,15]).

3.4. Measurement plan and strain history during setup

The twelve potentiometers (P1–P12) and three LVDTs (D1–D3) were connected to the specimen 1 and four additional LVDTs were used in specimen 2 (D4–D7) (Fig. 9). For the specimen with tension-

Table 3
Mechanical properties.

Name	Element	JIS coupon Shape	Thickness t (mm)	Yield strength σ_y (Mpa)	Tensile strength σ_u (MPa)	Elongation EL (%)
C-A	Infill panel	JIS 1B	1.60	201.9	329.6	34.4
C-B	VBE web	JIS 1A	5.61	328.9	438.1	28.0
C-C	HBE web	JIS 1B	6.88	343.4	482.1	19.9
C-D	VBE flange	JIS 1A	8.63	299.7	430.1	28.7

Name	Element	Average sensitivity kN/$\mu\varepsilon$	Yield strength kN	Tensile strength kN
C-F	Rod + turnbuckle	0.0864	60.5	81.5

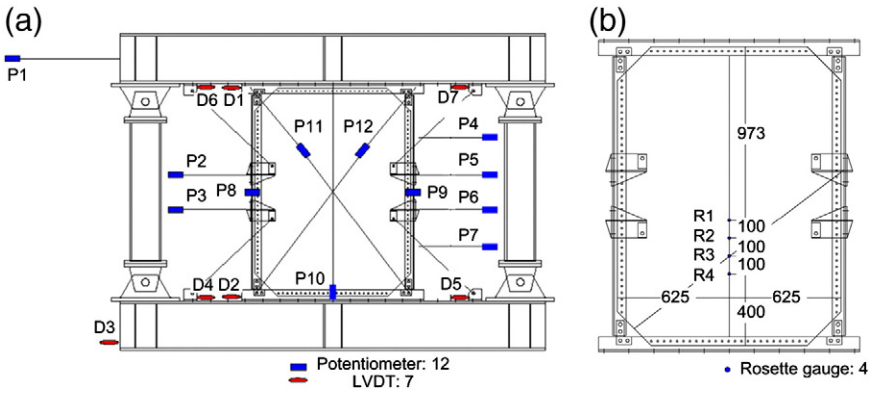

Fig. 9. Measurement plan for specimen 2: (a) LVDT and potentiometer; (b) strain gauges.

bracing (specimen 2), forces in the tension-bracings were monitored using uniaxial strain gauges attached on the turnbuckles. The relationship between the strain and the axial load in the turnbuckles were calibrated from preliminary tension tests so that the turnbuckles could be used as load cells (Table 3). The strain histories in the center part of the infill panels during the welding process were monitored using rosette strain gauges and uniaxial strain gauges (Fig. 10). The maximum principal strain values during the welding were around 230 $\mu\varepsilon$ and 175 $\mu\varepsilon$, for specimen 1 and specimen 2, respectively. These values were 10% of the yield strain, and much smaller than the values of the residual stress accounting for the column buckling strength (30% of the yield stress) in the modern steel design guidelines [11].

3.5. Test results and discussion

3.5.1. Specimen 1

The photos in Fig. 11(a) show the overall behavior and local damage of specimen 1. Global buckling of the infill plate took place immediately in the first load cycle with the amplitude of 0.00375 rad, with the development of tension field action in the infill plate. The buckling of the plate involved a single low tone sound following a series of high tone sounds accompanied by vibration of the infill plate. The main wave line in the global buckling ran exactly diagonally across the corners in the infill. The infill plate at the corner was subjected to compressive stress and was deformed out-of-plane. This out-of-plane deformation caused the weld metal at the boundary to be loaded under combined tension and shear. The two welds at the left bottom and the right top of the boundaries fractured during the second half cycle at 0.01 rad. Beginning at the 0.02 rad loading cycle, the VBEs deformed inelastically due to the inward force generated by the tension field action of the infill panel. At the left bottom corners of the infill panel, most of fractures occurred in the welds but some of them occurred in the base material (infill plate). Under further loading, fractures at the boundary connection propagated rapidly, with the bottom boundary of the infill panel almost disconnected at the end of the 0.04 rad loading. After the scheduled loading cycles were completed, a monotonic loading was applied to the specimen until the bottom boundary of the infill panel completely disconnected at the amplitude of 0.053 rad.

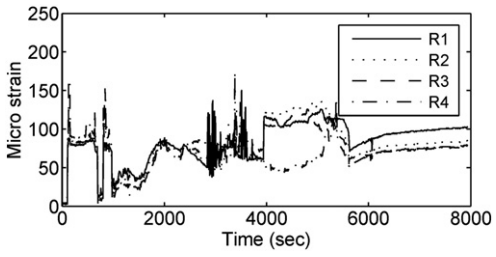

Fig. 10. Maximum principle strain in infill panel of specimen 2 during welding process.

Fig. 11(b) shows the global hysteresis behavior of specimen 1. The strength of specimen 1 reached its maximum value, 108 kN, during the first loading cycle at 2.0% story drift. The strength started to deteriorate slightly earlier (1.5% story drift) for the negative loading due to the fractures that propagated at the left bottom of the boundary connections.

3.5.2. Specimen 2

The photos in Fig. 12 show the overall behavior and local damage of specimen 2. As for specimen 1, global buckling of the infill plate took place immediately (*i.e.*, in the first load cycle at the 0.00375 rad) with the development of tension field action in the infill plate. However, the deformed shape exhibited more short wave lines for specimen 2 than for specimen 1, which indicated that the buckling mode was higher for specimen 2 than for specimen 1. The main wave line in the global buckling ran diagonally across the corners in the infill panel while two other wave lines initiated from the location of the steel brackets. Again, the buckling of the plate was accompanied by a single low tone sound following a series of high tone sounds with vibration of the infill plate. The rotation at the HBE–VBE connection was smaller than that in specimen 1, and the deformation at the corners of the infill panel was not large. As deformations became larger, the number of wave lines increased. This is because the tension-only bracing started to resist against the inward deformation of the VBEs and the tension load paths in the infill panel changed. The deformations at the corners of the infill panel were still limited as a benefit of the tension-bracing. No damage was observed at the boundary connections at end of the 0.01 rad loading cycle. At the 0.01 rad loading cycle, large deformations were observed in the steel brackets. Additional yielding of the steel brackets and yielding of the VBE occurred due to the large local force input from the tension-bracing in the 0.015 rad loading cycle. The steel bracket located at left bottom fractured during the 0.03 rad loading cycles. This undesirable fracture resulted in a slight buckling of the tension-bracing located at the bottom left. The yielding of all steel brackets affected the mode of the inelastic buckling and the deformed shape of the infill panel. This increased the force input in the corner of the infill panel and resulted in fractures at the bottom boundary connection. Under further loading, fractures at the bottom boundary increased excessively.

The strength of Specimen 2 reached its maximum value, 175 kN, during the first loading cycle at 3.0% story drift. The strength stopped increasing earlier in the positive loading due to early, undesirable yielding of the steel brackets at their left top and right bottom locations. The design of the steel brackets should be reexamined to prevent this early termination of the strength increase. At 3.0% story drift, the strength deterioration in the positive loading direction became significant due to the fracture of the steel brackets and the

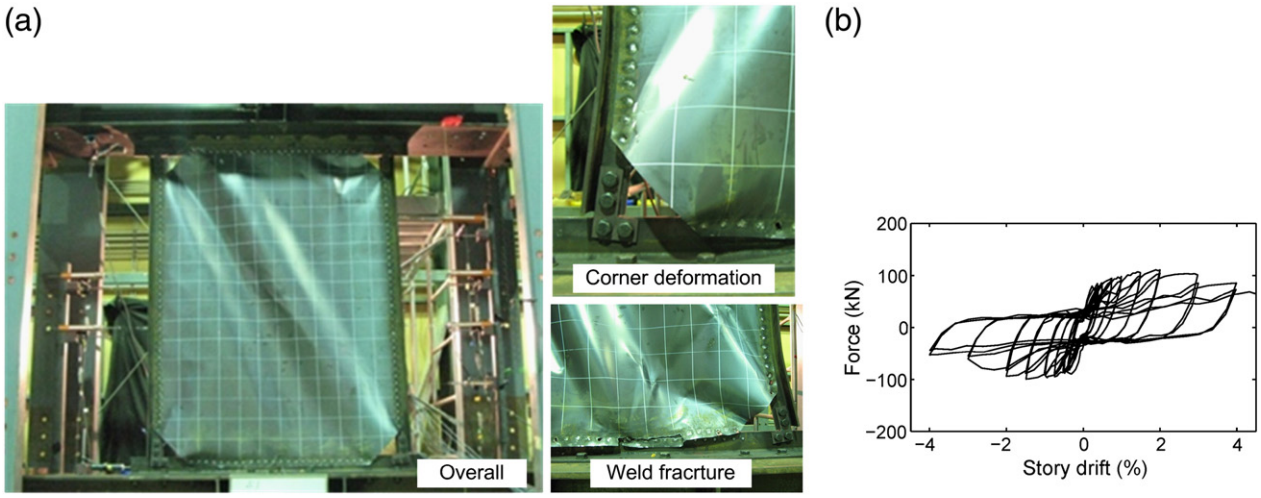

Fig. 11. Test results of specimen 1: (left) oveall behavior at 0.02 rad and local behavior; (right) force deformation relationship.

development of the yielding line in the flange of the VBEs. In the negative loading direction, the deterioration was milder where the steel brackets deformed in a rather ductile manner without fracture at the welds.

3.5.3. Comparison

When the two specimens were compared, the maximum strength was 62% larger in specimen 2 [Fig. 13(a)]. The ductility of the specimens, defined as the deformation where strength deteriorated to 80% of the maximum strength divided by the deformation at yield, were roughly estimated as 10 (2.5%/0.25%) for specimen 1 and 14 (3.5%/0.25%) for specimen 2; the deformation at yield were estimated from the bi-linearization of the strength envelop in the test results. The yield and maximum strength of both systems were around 10–15% smaller than the prediction analyses mainly due to damage in the welds at boundary elements which were treated as rigid in the simplified analyses. The energy dissipated by the two specimens did not differ much until 1% story drift [Fig. 13(b)]. This fact indicates that the tension-bracing contributed to stiffness and strength of the specimen 2 without adding much energy dissiapting capacity to the system. The difference of the amount of dissipated energy between two specimens increased notably after 1% story drift and reached approximately 30% of the energy dissipated by specimen 1 at a 4% story drift. The difference was mainly achieved by the energy dissipated by the steel brackets and VBEs and by the more ductile behavior of the infill panel in specimen 2 given the smaller damage at the boundary connection.

4. FE model calibration

The global and local behavior of specimens observed in the experimental study of the specimens was traced using a general-purpose

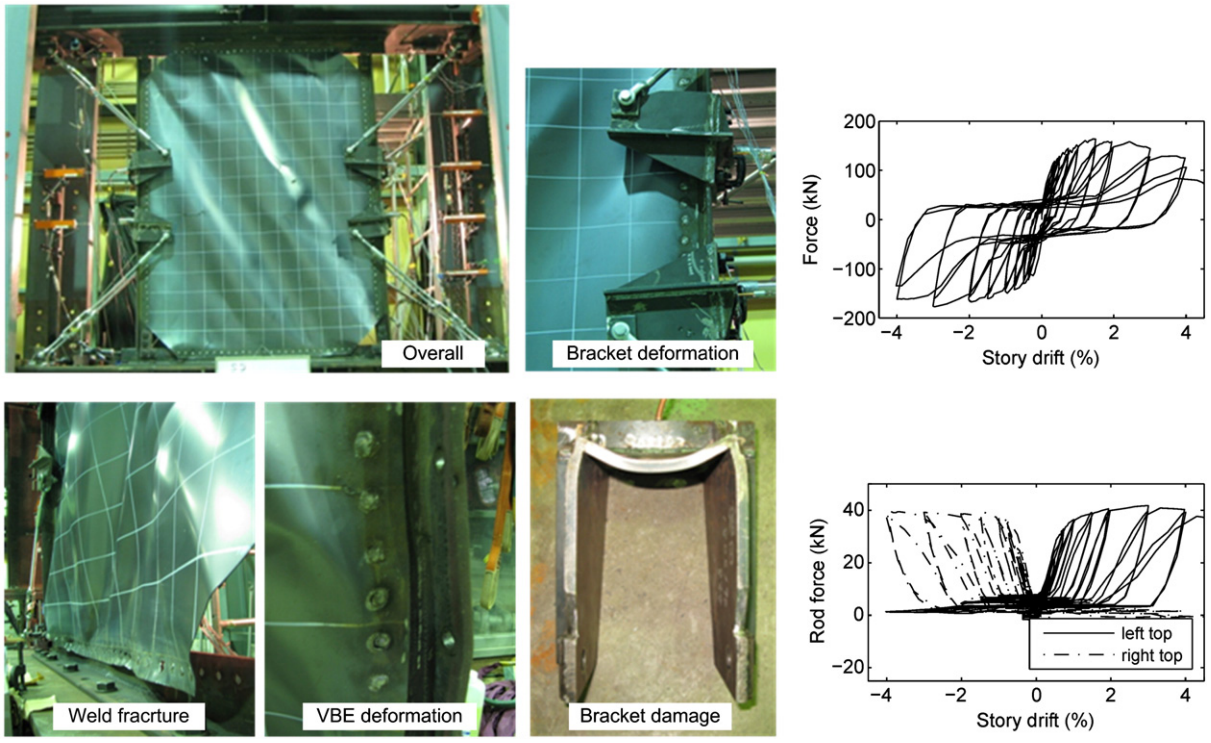

Fig. 12. Test results of specimen 2: (left) photos from test views; (right top) force deformation relationship; (right bottom) force history in tension rods.

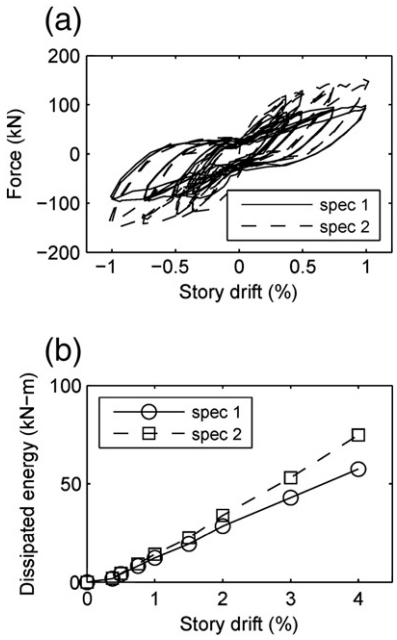

Fig. 13. Comparison of test results from specimens: (a) hysteresis until large deformation; (b) cumulative dissipated energy.

finite element program, ABAQUS [25]. The purpose of the high-fidelity FE model was to provide the accurate estimates in the design of the proposed system and check the accuracy of the preliminary prediction using the simplified analysis model. The specimens were analyzed together with the test setup used in the experiments.

4.1. FE model

Fig. 14 shows the analysis model constructed in ABAQUS. The bottom beam was ignored in the system; the bottom boundaries such as bottom pins and the flanges of the bottom HBE were fixed instead. The VBE, HBE, and the beam and columns in the test setup were modeled using a general-purpose four-node, doubly curved, finite membrane strain shell element (S4R) with reduced integration and linear geometric order. A two-node linear truss element (T3D2) was used for the modeling of the tension-rods. The HBE–VBE connections were modeled by assigning rigid body constraints at the end part of the VBE and HBE; only in-plane relative rotation is allowed for the VBE and HBE at the connection. The arms were modeled by rigidly connecting the ends of the tension-rods and the flanges of the VBEs using beam connectors; the arm inelasticity was not considered in the model. The beam-column connections were modeled by the combined use of beam and link connectors. To capture the non-linear behavior at the weld connection in the tests, the model included the detailed representation of weld connection at boundaries. Each pre-holed fillet weld was modeled by a general-purpose, four-node linear tetrahedral solid element (C3D4). The infill panel and the boundary elements were rigidly connected to the fillet weld model using the tie constraint feature. The top HBE was connected to the bottom flange of the top beam again using the tie constraint feature. The mechanical properties measured in the coupon test were used in the analyses. The infill panel and the fillet welds were modeled tri-linear with no strain hardening after plastic strains of 20% and 0.3%, respectively.

4.2. Finite element (FE) analyses results

Displacement-controlled pushover analyses up to 3.0% story drift and cyclic analyses at 1.0% story drift were executed. For specimen1, both the pushover and cyclic curve traced the experimental behavior very well [Fig. 15(a)]. The initial stiffness, yield strength and maximum strength predicted by FE model had good agreement with those observed in testing, even though the model did not include any deterioration behavior due to weld fractures. The cyclic analyses succeeded in tracking the strain softening after the load reversal due to the reversed global buckling of the infill panel. The FE model for specimen 2 well predicted the initial stiffness and the maximum strength but overestimated the yield strength by 30% [Fig. 15(b)]. The reason for the poor estimates in the yield strength was likely attributable to the early deterioration of steel brackets observed in the experiments. The under-designed steel brackets added the flexibility to the hysteresis curve before the yielding of the infill panel and fractures of the fillet welds. The monotonic curve included slight deterioration at large deformations mainly due to the yielding of the VBEs where the steel brackets are connected. The cyclic curve well traced the strain softening after the reverse of the loading direction. The force of one of the two rods at the right bottom under monotonic loading is also presented. The rod force showed excellent correlation

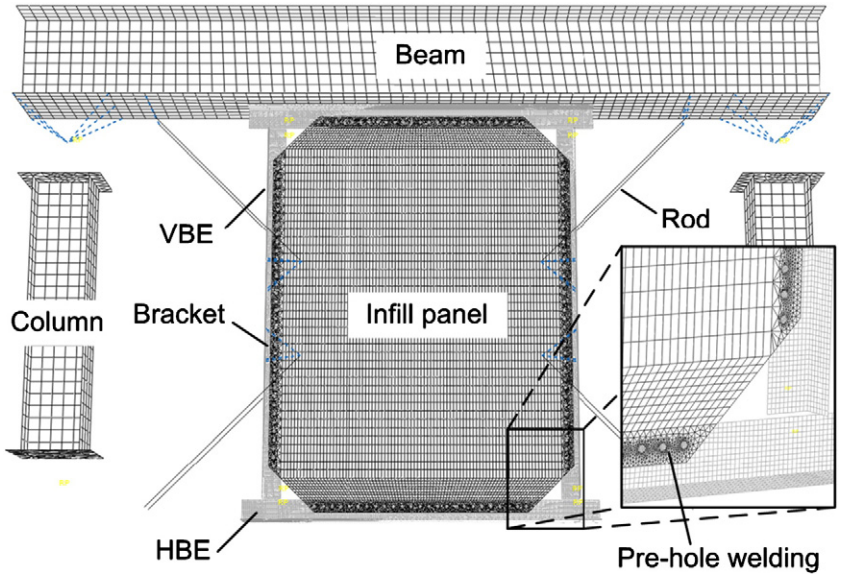

Fig. 14. FE model of specimen 2.

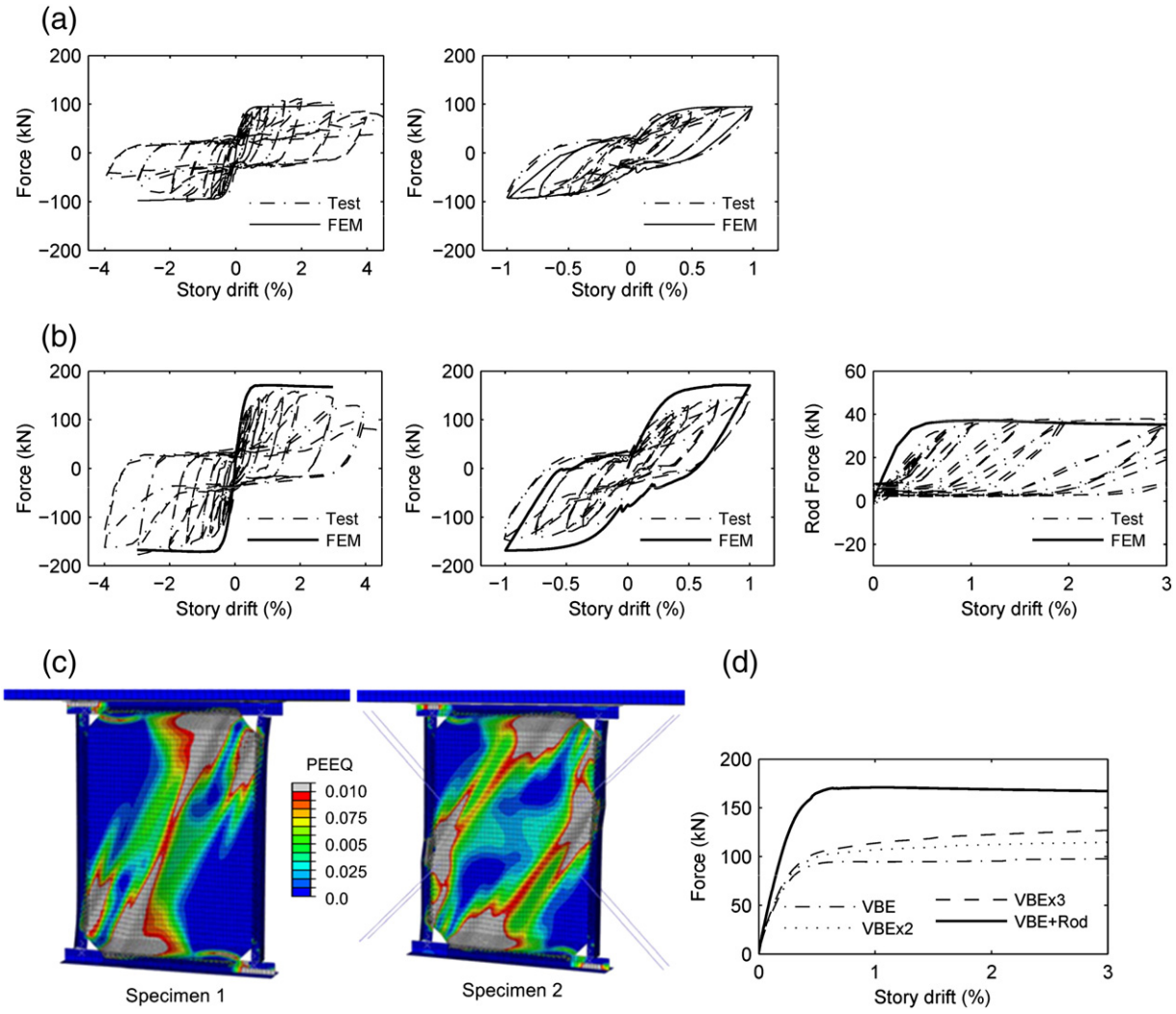

Fig. 15. FE model validation and parametric study: (a) specimen 1, (left) pushover curve, (right) cyclic prediction; (b) specimen 2, (left) monotic prediction, (right) cyclic prediction; (c) deformed shape of specimens with plastic strain contour (PEEQ) at 3% story drift; (d) VBE parametric study.

with the test result. Fig. 15(c) illustrates the development of tension field action in the infill panels and the amount equivalent plastic strain (*PEEQ*). With the presence of the tension-bracings, the inclination of tension filed was larger and the larger area of the infill panel was subjected to yield.

A parametric study on the strength and stiffness of the VBEs were conducted using the developed high-fidelity FE model. Four models were prepared: 1) specimen 1 (named VBE); 2) a model with double thickness for VBE web and flange (named VBE×2); 3) a model with triple thickness for VBE web and flange (named VBE×3); and 4) specimen 2 (named VBE + Rod). The monotonic loading of four models showed the clear advantage of adding the tension-rods over increasing the sectional dimensions and weights of the VBE with significantly higher stiffness and yield strength (Fig. 10). The small or slightly negative post-yielding stiffness helps limit the force demand to the surrounding frame and is well suited to the strict capacity design principle.

5. Conclusions

A supplemental shear wall system with a steel thin plate is proposed for the rehabilitation of small to mid-sized steel frame. In the system, the plate and surrounding boundary elements are installed in the middle of the bay, separate from existing columns to eliminate the need to strengthen these elements. The system employs an approach to design supplemental elements as tension-only to speed up the construction work and to obtain a strict capacity design. A prototype system was hierarchically designed using a design flowchart and a simplified analysis model and was evaluated through large scale testing. A high-fidelity FE model of the system was also developed to reproduce the experimental behavior. The key findings and conclusions are summarized as follows:

1. The prototype system successfully reflected the design philosophy by following the hierarchy of yielding modes in the design flowchart.
2. In testing, the prototype system behaved as intended in the design. The yield strength and initial secant stiffness were increased by approximately 45% by the addition of the tension-bracing. The tension-bracing contributed to the increase of shear strength at the 0.01 rad and at peak by 67% and 62%, respectively.
3. Strength started to deteriorate much later with the presence of the tension-bracing. In the case without the tension-bracing, the strength started to deteriorate slightly at the 1.5% story drift due to the fractures that propagated at the left bottom of the boundary connections. In the case of the tension-bracing, the strength deterioration in the positive loading direction became significant at the 3% story drift, due to the fracture of steel brackets and the development of the yield lines in the flange of the VBEs. The ductility of the specimens, defined as the deformation where strength

deteriorated to 80% of the peak strength divided by the deformation at yielding, were roughly estimated as 10 and 14 for specimens with and without tension-bracing, respectively.

4. The FE model of the prototype well traced the experimental behavior in pushover and cyclic analyses. The parametric study using the model concluded the enhanced effectiveness of adding tension-bracing over increasing the sectional properties of the VBE.

Acknowledgments

The authors would like to thank Dr. A. Jacobsen and Mr. Shiga for their advice and invaluable support of the experimental program at Kyoto University.

References

[1] Kurata M. Strategies for rapid seismic hazard mitigation in sustainable infrastructure systems. PhD's thesis. Georgia Institute of Technology. Atlanta. Georgia; 2009.
[2] Kurata M, Leon RT, DesRoches R. Rapid seismic rehabilitation strategy: concept and testing of cable bracing with couples resisting damper (CORE damper). J Struct Eng 2011 Posted ahead of print 18 February.
[3] Thouburn LJ, Kulak GL, Montgomery CJ. Analysis of steel plate shear walls. Struct Eng Report, 107. Canada: Dept of Civil Eng. University of Alberta; 1983.
[4] Tromposch EW, Kulak GL. Cyclic behavior of thin panel steel plate shear walls. Struct Eng Report, 145. Canada: Dept of Civil Eng. University of Alberta; 1987.
[5] Sabouri-Ghomi S, Roberts TM. Nonlinear dynamic analysis of steel plate shear walls including shear and bending deformations. Eng Struct 1992;14(3):309–17.
[6] Caccese V, Elgaaly M, Chen R. Experimental study of thin steel-plate shear walls under cyclic load. J Struct Eng 1993;119(2):573–87.
[7] Elgaaly M. Thin steel plate shear walls behavior and analysis. Thin Walled Struct 1998;32:151–80.
[8] Behbahanifard M, et al. Experimental and numerical investigation of steel plate shear walls. Struct Eng Report, 254. Canada: Dept of Civil Eng. University of Alberta; 2003.
[9] Sabelli R, Bruneau M. Steel plate shear walls. Steel Design Guide 20. Chicago. Illinois: American Institute of Steel Construction, Inc.; 2006.
[10] Canadian Standard Association. S16-01-CAN/CSA: limit states design of steel structuresSixth edition. ; 2006. Toronto. Canada.
[11] American Institute of Steel Construction. Seismic provisions for structural steel buildings; 2007. Chicago, Illinois.
[12] Lubell A, Prion HGL, Ventura CE, Rezai M. Unstiffened steel plate shear wall performance under cyclic loading. J Struct Eng 2000;126(4):453–60.
[13] Qu B, Bruneau M, Lin CH, Tsai KC. Testing of full-scale two-story steel plate shear wall with reduced beam section connections and composite floors. J Struct Eng 2008;134(3):364–73.
[14] Berman JW, Bruneau M. Experimental investigation of light-gauge steel plate shear walls. J Struct Eng 2005;131(2):259–67.
[15] Vian D, Bruneau M. Steel plate shear walls for seismic design and retrofit of building structures. Technical Report MCEER-05-0010. SUNY Buffalo. New York: MCEER; 2005.
[16] Roberts TM, Sabouri-Ghomi S. Hysteretic characteristics of unstiffened perforated steel plate shear panels. Thin Walled Struct 1992;14:139–51.
[17] Purba R, Bruneau M. Design recommendations for perforated steel plate shear walls. Technical Report MCEER-07-0011. SUNY Buffalo. New York: MCEER; 2007.
[18] Hitaka T, Matsui C. Experimental study on steel shear wall with slits. J Struct Eng 2003;129(5):586–95.
[19] Driver RG, Kulak GL, Elwi AE, Kennedy DJL. FE and simplified model of plate shear wall. J Struct Eng 1997;124(2):121–30.
[20] Mazzoni S, McKenna F, Scott MH, Fenves GL. Opensystem for earthquake engineering simulation: user command language manual. University of California, Berkeley: Pacific Earthquake Eng Research Center; 2006.
[21] Rezai M. Seismic behavior of steel plate shear walls by shake table testing, PhD dissertation. Dept of Civil Eng. University of British Columbia. Vancouver. Canada; 1999.
[22] Wakabayashi M. Steel structures. Tokyo: Maruzen; 1985 (in Japanese).
[23] Building Center of Japan (BCJ). Steel deck 2004. Japan Iron and Steel Federation (JISF); 2004.
[24] Japanese Industrial Standards (JIS). G3136-05: rolled steels for building structure; 2005.
[25] Dassault Systems. ABAQUS version 6.8 documentation. Velizy-Villacoublay France: Dassault Systems; 2008.